Korean J. Chem. Eng., 32(9), 1928-1937 (2015)
DOI: 10.1007/s11814-015-0004-3

pISSN: 0256-1115
eISSN: 1975-7220

Morphology study of nanofibers produced by extraction from polymer blend fibers using image processing

Neda Dehghan, Mohammad Ali Tavanaie†, and Pedram Payvandy

Textile Engineering Department, Faculty of Engineering, University of Yazd, P. O. Box 89195-741, Yazd, Iran
(*Received 27 September 2014 • accepted 1 January 2015*)

Abstract−The morphology of nanofibers extracted from the industrial-scale produced polypropylene/polybutylene terephthalate (PP/PBT) blend fibers was studied. To study the morphology and diameter measurements of the nanofibers, image processing method was used, and the results were compared with the results of a conventional visual method. Comparing these two methods indicated the good performance of image processing methods for the measuring of nanofiber diameter. Among the various applied image processing methods, the fuzzy c-means (FCM) method was determined as the best for image thresholding. Additionally, the distance transform method was determined as the best way for measuring nanofiber diameter. According to high regression coefficient (R=0.98) resulting between the draw ratio and nanofibers diameter, the high effectiveness of draw ratio to nanofiber diameter is concluded. The spherical (drop) shapes of the PBT dispersed phase particles were eventually deformed into very thin fibrils during the drawing process. The results of measuring the nanofiber diameters showed that the diameter means of nanofibers varied from 420 nm to 175 nm with the highest draw ratio. Good uniformity for diameter of nanofibers was observed, which had not been observed in previous works.

Keywords: Polymer Blend Fibers, Nanofibers, Morphology, Draw Ratio, Image Processing

INTRODUCTION

The main purpose of blending polymers is to obtain materials suitable for specific needs by creating or improving one or more properties with minimum destruction in other properties. Different shapes of dispersed phase (as minor phase) such as sphere, laminar and fibrillar may form in the matrix phase (as major phase) of polymer blends. Production of blend fibers during the melt spinning can result in more effective fibrillar phase morphology than in other methods because of the existence of elongational force field, which are also called matrix-fibrill fibers [1]. In a matrix-fibril fiber, the fibrils are placed randomly within the matrix. By dissolving the matrix component, a set of very thin fibrils is obtained [2].

Recently, many researchers have focused on micro- and nanofibril formation in the matrix phase of immiscible blend fibers [3-6]. The processing parameters and characteristics of polymers affect the size of fibrils. Some of these factors are various rheological and processing factors. These parameters include the viscosity ratio of components [2], the blend ratio of component [7], the presence of compatibilizer agent [8,9], the type of flow field (whether shear or elongational) [10], the type of dispersed or matrix component, stress rate, extrusion temperature, winding or take-up speed, etc. [1].

Drawing operation is conducted to obtain the desired characteristics of the fibers during or after the fiber formation process. This operation makes appropriate values o f tensile and structural properties such as elongation at break, tenacity, orientation and the crystallinity of fibers in terms of their final consumption [11]. The length over diameter ratio of the dispersed phase particles could be increased by drawing blend fibers. Furthermore, these particles could be changed to microfibrils and even nanofibrils by drawing operation [12,13]. The fibrils had a wide range of sizes, considering their production methods.

The drawing operation can be performed in two ways: in hot (feeding roller at a temperature higher than the glass transition temperature (T_g) (for both polymers)) and cold conditions. Cold drawing creates aligned fibrils into the matrix phase of blend fibers. Moreover, hot drawing can makes a possible higher draw ratio of blend fibers compared to cold drawing [9]. Often with the increase of draw ratio, in addition to decreasing fibril diameter, the uniformity of the fibrils length increases [1]. Changes in the morphology of micro- and nanofibrils resulting from blend fibers were studied by various researchers [9,13,14].

Jayanarayanan et al. observed that fibril diameter in dispersed phase of the PP/PET injection molded composite decreases with increasing of the draw ratio [14]. Bagheban et al. [9] observed that polypropylene dispersed phase particles deform during the drawing process. Their fibril diameters in the blends with compatibilizer agent were smaller and more uniform, compared to the blend without compatibilizer agent. The diameter of the thinnest fibril was around 300 nm.

Falahi et al. studied the production of nanofibrils from a PP/PA6 blend fiber. They observed that fibrils were oriented toward the drawing direction, whichever the ratio of undrawn fibrils mean diameter over drawn fibrils mean diameter was reported as 1.2. A wide range of 300 nm to 1,200 nm was also reported for fibril diameter [13].

†To whom correspondence should be addressed.
E-mail: ma.tavanaie@yazd.ac.ir

Other presented results considered one of the most important morphological characteristics of nanofibers to be their diameter evaluation. Diameter of nanofibers is typically measured by the scanning electron microscopy visual method. Therefore, researchers have previously paid attention to providing ways for evaluation of the precise average fibril diameter with SEM images [15-19]. Pore size is another important property of nanofiber layers that previously was studied using image processing [20,21].

Shin et al. [15] used an image processing method to determine the diameter of electrospun nanofibers. Distance from the center towards the edges of the fiber was calculated using the distance transform method. Ziaberi et al. [16,17] suggested a new distance transform method for measuring the diameter of electrospun nanofibers. By identifying the intersections of fibers and removing them from the image of the object skeleton, this method measures the distribution of fiber diameter more precisely. Also, they suggested a direct tracking method for measuring electrospun nanofiber diameter [18].

Electrospinning has many limitations and the possible non-uniformities of nanofibers. So, production of the nanofibers from polymer blend fibers is considered to be a new approach with many advantages: for example, higher production speeds, lower production costs, and more flexibility in the production of nanofibers with different diameters and more uniformity. In the present study, nanofiber layers were produced by extracting dispersed phase fibrils from the matrix of the polypropylene/polybutylene terephthalate (PP/PBT) blend fibers. Also, the surface morphology of nanofiber layers was studied using an image processing method.

EXPERIMENTAL

1. Materials

PP/PBT polymer blend fibers (as the shape of multifilament yarn) with low orientation (LOY) produced at industrial conditions were used. Manufacturing conditions are presented in Table 1. In the undrawn as-spun fiber production stage, the presence of a 10% PBT dispersed phase content did not significantly affect the spinning characteristics of the fibers, and using a 1% polypropylene-grafted-maleic anhydride (PP-g-MAH) as a compatibilizing agent caused the desired compatibility of the two components and the production of blend fibers with appropriate elongation at break. Note that the presence of the PBT in modified fibers increased the elongation at break of the as-spun blend fibers, and consequently increased the draw ability of the blend fiber samples [22]. Xylene was used as a suitable matrix phase solvent for extraction of the nanofiber layers from the blend fiber samples.

Table 1. Melt spinning specifications of the PP/PBT blend fibres (as a multifilament yarn form) at industrial conditions

Amounts	Parameter (units)
20	Extruder screw speed (rpm)
260	Final temperature of extrusion, spinning head and spinneret (°C)
90	Melt pressure at output of the extruder (bar)
8	Gear pump (rpm)
19	Cooling air temperature (°C)
0.3	Cooling air speed (m/min)
800	Winding speed (m/min)
17	Number of spinneret holes

2. Methods

The PP/PBT blend fiber was melt spun at industrial conditions in Aliaf Co. (Iran). The melt spinning line was equipped with an extruder model 4E6 (manufactured by Barmag Co., Germany) with a screw length over diameter ratio (L/D) of 24, and included a gear pump with a capacity of 0.8 ml per round (manufactured by Zenite Co., Germany) a spinneret with circular hole (manufactured by Elmer Co., Germany) and low speed winding machine (manufactured by IWKA, Germany).

The drawing process was conducted using a tensile testing machine, model SDL micro 350 (manufactured by SDL International Ltd./Shirley Development Ltd., UK). This machine works based on a constant rate of elongation equipped with a load cell of 10 kgf. A Projectina microscope was used to observe and measure the blend fiber diameter. To study the nanofiber layer morphology, a scanning electron microscope (manufactured by Tescan Co., Czech) was used. Nanofiber layer images with a magnification of 5000, 10000, 15000 and 30000 were prepared and analyzed.

Drawing process was carried out up to the maximum drawability of the fiber samples (draw ratio=4). Twelve draw ratios were applied to the fibers from 1.25 to 4 at the intervals of 0.25, i.e., 1.25, 1.5, 1.75, 2, 2.25, 2.5, 2.75, 3, 3.25, 3.5, 3.75 and 4, respectively. The undrawn PP/PBT blend fiber was used as the initial sample. Fig. 1 presents the process schematic of PP/PBT blend fiber production and their drawing process to deform the PBT dispersed phase parti-

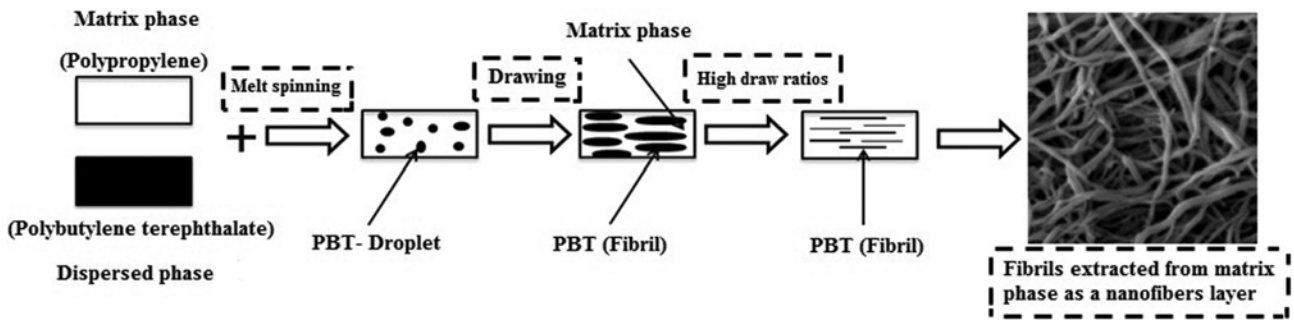

Fig. 1. Schematic of the nanofibres layers production method.

cles into fibril form, and finally extracting the nanofibrils by dissolving the matrix phase component.

To study the appropriate methods for producing nanofibers by extraction method, the blend fiber samples were dissolved for 30, 45 and 120 minutes to determine the optimal time at which the phase component is dissolved and the dispersed phase is formed as a layer of nanofibers. The extracted layers were placed at room temperature for 24 hours until they were completely dried and the solvent was removed. A sample weighing method was used before and after dissolving the component; then, images of the samples were provided by SEM in order to find their dissolution rate as well as the effect of variously applied draw ratios. A xylene solvent was used to dissolve PP at boiling temperature. The best time for dissolving the matrix phase component was 30 minutes.

Measuring of nanofiber diameters is highly important and complex due to their superfine diameters and various orientations. A visual method was considered improper, because of the need for using a human (operator) force, which should be replaced to measure the diameter of fibers accurately and quickly. For this reason, more recently, the image processing method has been applied for measuring. Choosing a suitable method for pre-processing the images and selecting a proper threshold for separating objects from the background are major stages during image processing. In this investigation, five different methods for image thresholding and two methods for measuring diameter were introduced.

3. Image Processing

Thresholding is a process in which a grey image is turned into a black and white image using an optimal threshold value. In thresholding, each pixel of the image is marked as either the object or the background. Each pixel is related to the object if the strength of the pixel is higher than the determined threshold value; and if it is lower than the threshold, it is related to the background. The thresholding method is generally divided into global and local thresholding [23]. Other methods used to threshold fuzzy algorithms include the k-means clustering algorithm, the fuzzy c-means (FCM) clustering method and the imperialist comparative algorithm (ICA) [24].

One threshold value is used for the entire image when applying the global threshold method. In the case of local thresholding rendering the clarity of the background unclear, dividing the image into smaller images makes the brightness of each part almost uniform.

One of the most important clustering algorithms is the FCM algorithm. In this algorithm, the pixels are divided into C (certain number) clusters [25]. Image features (intensity values) are used as input data to the algorithm. When pixels are closer to the center of their clusters, they have high membership value, while low membership value belongs to the pixels far from the center. Sivakumar applied the fuzzy clustering method for dividing mammogram images and introduced it as an appropriate method for sharing medical images [26]. K-means clustering or cluster analysis is a branch of data analysis science that contributes data to predetermined clusters. These clusters are defined based on common characteristics of data and without using any default data. Data consists of image details in which each cluster contains similar data dissimilar to data in other clusters. Various criteria can be considered for similarity; one of the most applicable criteria for clustering is distance. Then, the closer data is regard as one cluster. Another applied algorithm is a heuristic algorithm that divides the image according to the primary population and then applies a target function. This approach has been inspired by the k-means algorithm and image data [27].

Two methods are applied for measuring diameter: the image processing method (distance transform, direct tracking method) and the visual method. In the present study, Euclidean distance transformation was used to measure the diameter of nanofibers in the distance transform method. The direct tracking method was also one of the image processing methods used for measuring nanofibers diameter. In this method, the measured distance as radius is doubled to obtain nanofibers diameter. The visual method is the conventional method for measuring the diameter of fibers. First, a scale is set; then, pixels located between two edges of the vertical axis are counted. The number of pixels is converted to nanometers (nm) and the results are reported. Depending on the conditions of an image, 30 to 100 diameters could be measured. This method is time-consuming and requires an operator, which reduces its accuracy. Automated measurement of diameter and omitting a human (operator) force for measurement can be selected as a natural solution for solving this problem.

RESULTS AND DISCUSSION

SEM images of the thirteen nanofiber layers extracted from the undrawn and drawn PP/PBT blend fibers with different draw ratios are presented in Fig. 2.

In the presented images (Fig. 2), the diameter of dispersed phase particles was decreased by increasing of the draw ratio. As shown in the same images, it can be concluded that the production of nanofibers according to this method truly is possible. The shape of dispersed phase particles in undrawn nanofiber layer was almost ellipsoidal. The ellipsoidal shape of the particles was converted into completely drawn fibrillar shapes (nanofibril shape), by increasing the draw ratio. Accordingly, the dispersed phase component did not necessarily deform into complete fibrils in the presence of drawing fields during the process of fiber formation (melt spinning). Furthermore, the drawing fields intensively affected the deformation of the dispersed phase component following the freezing of fibers (during the melt spinning process or in a post-spinning stage). Notably, the increase of winding speed during the melt spinning process had the potential for leading to the formation of very thin and long fibrils. In this project, we used low oriented blend fibers to consider the possibility of producing different nanofiber fineness.

Table 2 presents the correlation coefficients of the mean of diameters for different applied methods. The correlation coefficient is a statistical indicator that indicates the presence or absence and intensity of the relationship between two variables. The correlation coefficients of the mean of diameters were calculated to determine the relationship between the mean of different methods. Accordingly, the results of the image processing method are close to the standard method, i.e., the visual method.

Significant coefficients for all methods were less than 0.05 (sig< 0.05), which means there was a relationship between variables. The correlation coefficient higher than 0.95 between visual and image

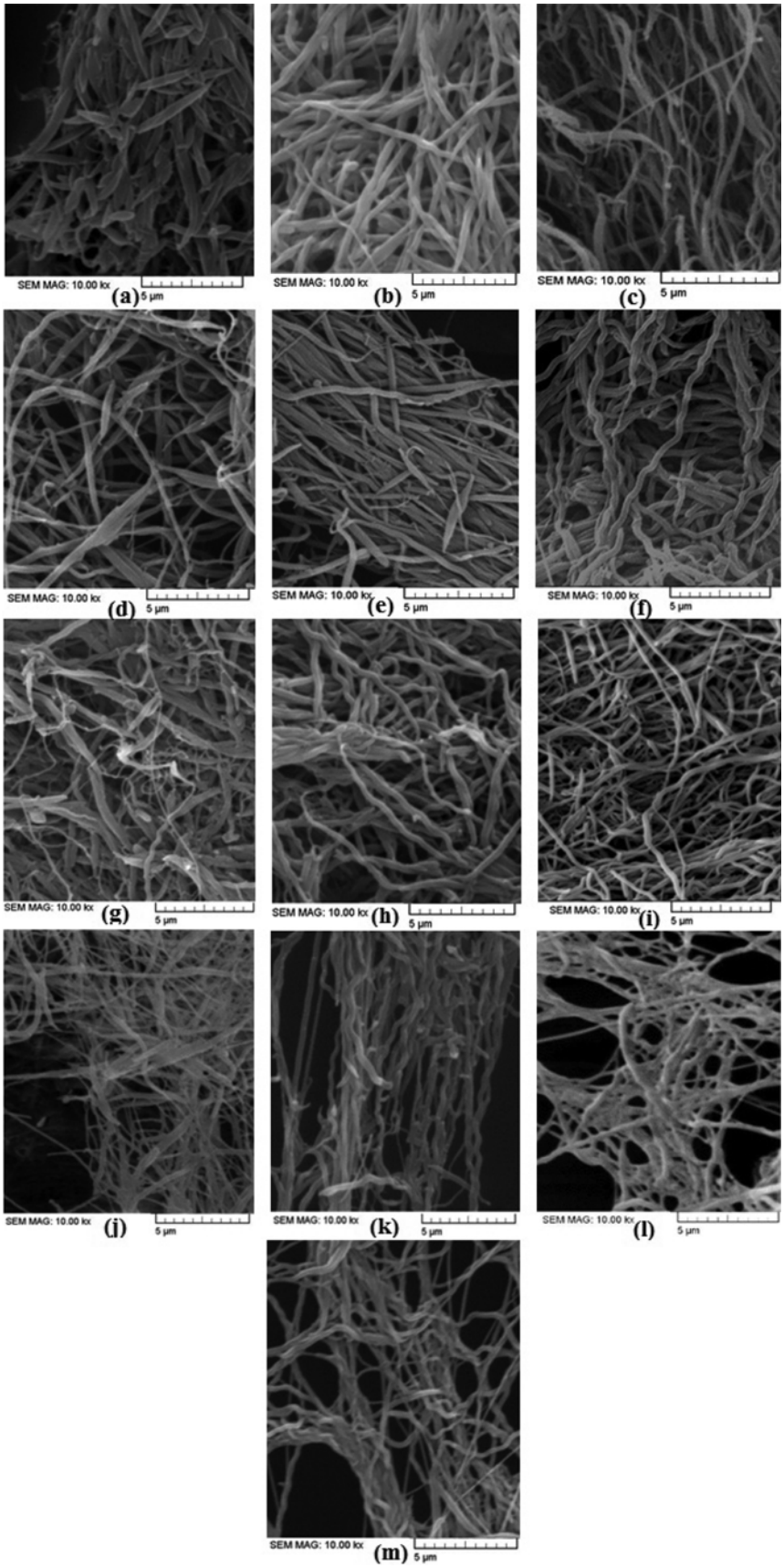

Fig. 2. Nanofibres layers extracted from the blend fibres samples drawn with different draw ratios: (a) 1, (b) 1.25, (c) 1.5, (d) 1.75, (e) 2, (f) 2.25, (g) 2.5, (h) 2.75, (i) 3, (j) 3.25, (k) 3.5, (*l*) 3.75, (m) 4.

Table 2. Correlation coefficients between the mean of nanofibres diameters measured with different methods

Thresholding method-diameter measurement method	Visual method correlation coefficient
Otsu-Distance Transform	0.966
Otsu-Direct Tracking	0.977
Local-Distance Transform	0.984
Local-Direct Tracking	0.977
K-means- Distance Transform	0.989
K-means- Direct Tracking	0.984
FCM- Distance Transform	0.992
FCM- Direct Tracking	0.984
ICA- Distance Transform	0.988
ICA- Direct Tracking	0.965

processing methods indicates a strong and positive relationship between these methods and the visual method. The highest correlation coefficient for the diameter determining method was for distance transform. Among thresholding methods, the best method with the highest correlation coefficient was the fuzzy c-means (FCM).

In the fuzzy method, an object belongs to all clusters with different degrees of membership, and when the data are overlapping, this method provides the best tool for clustering the data. In the case of nanofiber layers images, the best division is done through FCM. Then, in order to measure nanofibers diameter, the image processing method was applied, FCM was applied for thresholding, and the distance transform method was applied for measuring diameter. Fig. 3 shows the image of thresholding using FCM for nanofiber layers with a draw ratio of 4.

The thresholding image of Fig. 3 shows that the thresholding method was suitable for distinguishing nanofiber layers from the background. To measure diameter using the distance transform method, the image was divided into sub-images. All nanofiber layers were measured by the FCM thresholding method and two diameter measuring methods: the distance transform and visual method.

The results of diameter measurement were analyzed. As an example, the results of the measured diameters of three samples of the nanofiber layer (undrawn sample, sample with the draw ratio of 2 and sample with the draw ratio of 3) are presented in the form of a normal curve by image processing and visual methods. Fig. 4 shows the results of the three samples with different draw ratios as normal frequency curves with mean and standard deviation, as well as the numbers of measured diameters.

As can be seen in Fig. 4, the visual and image processing methods had a normal distribution curve; these methods had a frequency along the entire range of the measured diameters. Frequency distribution curves for the visual method had a normal and uniform distribution. However, these distribution graphs were not uniform in the previous research, and for some draw ratios no frequency were observed [9, 12]. The more uniform distributions results of this study can be related to the resulted uniformity of the blend fiber produced in industrial conditions of this work compared to other blend fibers produced at laboratory scale [9,12,13].

As can be seen in the curves presented in Fig. 4, the mean of diameter was similar for both methods. The mean of diameters of the thirteen nanofiber layers were calculated. Table 3 shows the mean of diameter for all samples which was measured with both methods.

As shown in Table 3, the obtained results from FCM and visual methods in all draw ratios are very close together and show a difference of 1.5% to 10.5%. Fig. 5 shows the mean of the measured diameters for the FCM and visual methods using the distance transform measuring method for all draw ratios. Generally, the results of the mean of diameters confirmed the decrease in fibrils diameter by increasing the draw ratio, as was previously noted.

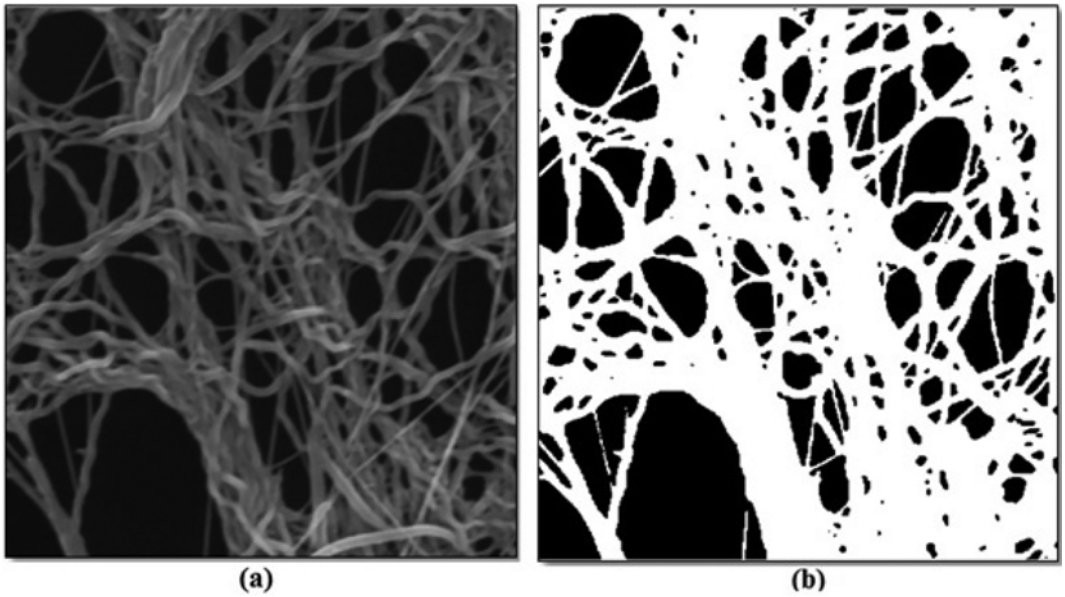

Fig. 3. Images of the nanofibres layer extracted from drawn PP/PBT blend fibres sample with the draw ratio of 4, (a) normal image, and (b) thresholded image by fuzzy c-means.

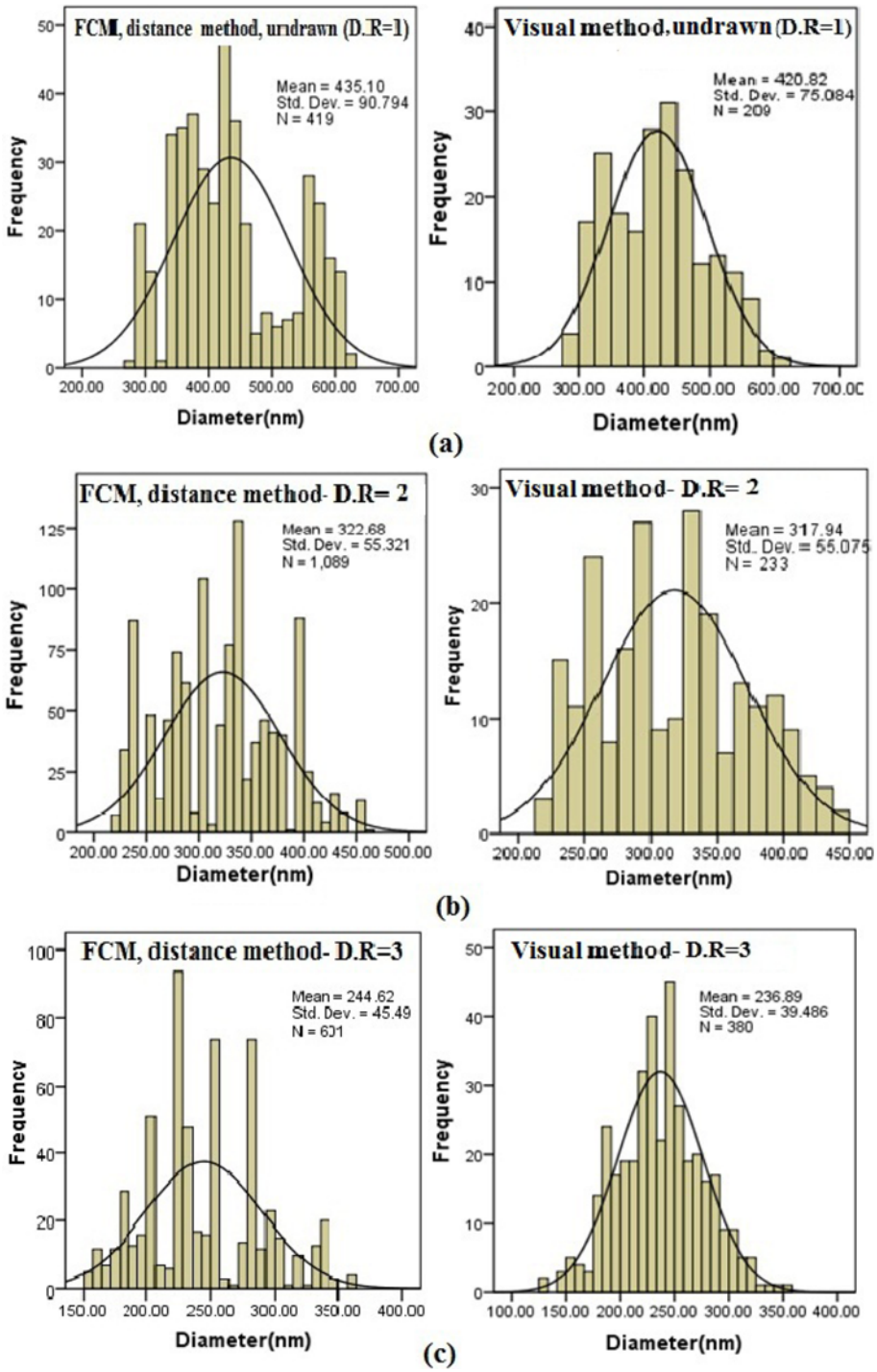

Fig. 4. Normal frequency curves of the measured diameter using visual method (on right), and fuzzy c-means- distance transform methods (on left), for different blend fibres samples: (a) Undrawn, and drawn with the draw ratios of (b) 2, and (c) 3.

According to Fig. 5 and Table 3, the smallest differences of diameters were obtained for draw ratios of 2 and 3.25. Totally, the difference between means of diameter was reduced with increasing the draw ratio and decreasing the nanofiber diameter. In all draw ratios, except in the draw ratio of 3.25, the determined diameter using the FCM method was greater than the determined diameter of the visual method. The maximum difference between the mean of diameters in both methods was 32.8 nm, which occurred in the draw ratio of 1.25. The greatest value for the diameter mean of nanofibers can be related to the nanofiber edge measured with FCM method, rather than in the visual method.

The mean of diameter variations in the different draw ratios are presented in Fig. 5. The mean of fibril diameters extracted from the undrawn and drawn PP/PBT fibers changed from 420 nm to

Table 3. Means of the nanofibres measured diameters with visual and image processing methods and the diameters mean of the blend fibres sample

Draw ratio	Mean of blend fiber diameters (nm)	Mean of nanofibre diameters-visual method (nm)	Mean of nanofibre diameters- FCM method (nm)
1	5600	421	435
1.25	4800	361	394
1.5	4000	350	382
1.75	3600	345	369
2	3200	318	323
2.25	3200	330	342
2.5	2800	311	327
2.75	2800	281	311
3	2400	237	245
3.25	2400	224	224
3.5	2000	209	232
3.75	2000	211	221
4	2000	175	188

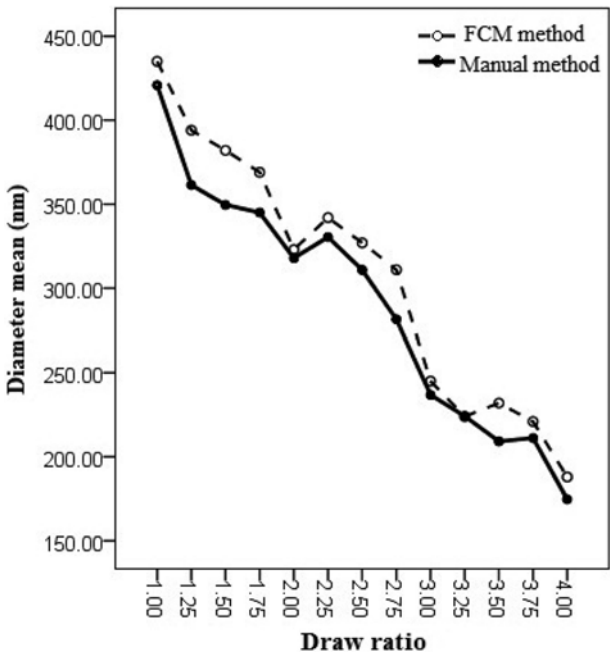

Fig. 5. Mean of the nanofibres diameters measured with visual and fuzzy c-means methods versus draw ratio.

175 nm for the visual method, and from 435 to 188 nm for the FCM method.

Very high fluctuations in the diameter of nanofibers were reported by many researchers; in some cases, these fluctuations were higher than 50% [9,28,29]. However, in the present research, very low fluctuations were observed: the average of 12% and the maximum of 20%. This is a highlighted advantage of using industrial-scale over laboratory-scale produced polymer blend fibers.

According to Fig. 5, the greatest changes in diameters with increasing the draw ratio were seen until the draw ratio of 1.75 for both

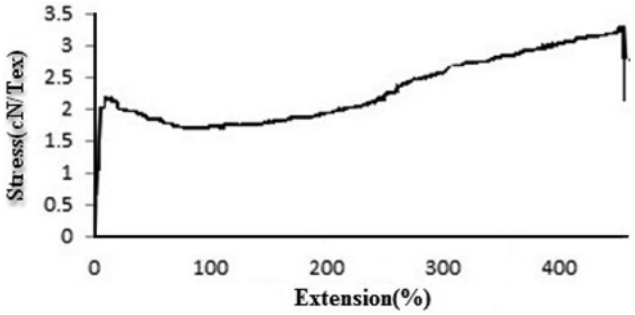

Fig. 6. Stress-strain curves of the undrawn PP/PBT blend fibres sample.

the visual and optimum image processing method. In the following draw ratios, the differences of both methods were in good agreement with each other. A decrease in the mean of fibril diameters in the draw ratio of 2 can be considered with the stress-strain curves of the PP/PBT blend fibers.

The stress-strain curve of the blend fiber sample is shown in Fig. 6. The stress-strain curve was associated with necking in the yield point and irreversible elongation in the plastic point and then in the hardening zone. Regarding Fig. 6, a point with 100% elongation was of minimum recorded force before breaking point, which was related to the draw ratio of 2. It was seen that the blend fibers sample under tensile load did not have enough resistance to load at low stresses. Consequently, the blend fiber sample showed a high elongation before the hardening point, and the highest and the most unexpected decrease in fibril diameter occurred in this ratio (D.R= 2). A regular diameter reduction was seen by increasing the draw ratio more than 2 due to increasing the resistance of the blend fibers to load from this point (the strain of 100%).

In other research [9], nanofibril morphology was studied based on SEM images obtained in various elongations. It was stated that the beginning of fibrillation of the dispersed phase particles happened in the final stage, and close to the breaking point of the fibers, i.e., when the matrix component transferred the maximum stress to the dispersed phase component. In the present investigation, through a more detailed morphological study of the samples in smaller draw ratios and by observing changes in the diameter of dispersed phase particles in different ratios, it was seen that the fibrillation of the dispersed phase started nearly from the yield point (draw ratio of 1.2). Also, the images of Fig. 4(a)-(m) show gradual changes in all draw ratios. There is a high strain in low stresses at the yield point. Other changes in particles' shape and diameter occurred in order to decrease the fibril diameter and increase their length following a draw ratio of 1.2.

The PP/PBT blend fiber sample was drawn using a tensile testing machine. Draw ratios, which were calculated from initial and final length of the tensile testing machine, were introduced as nominal draw ratio. Longitudinal deformation of the dispersed phase particles (fibrils) takes place within the matrix phase due to drawing the blend fibers. Table 3 presents the mean of blend fiber diameter in the range of microns. The actual draw ratio of the blend fibers was calculated by dividing the undrawn fiber diameter over its diameter after the drawing operation.

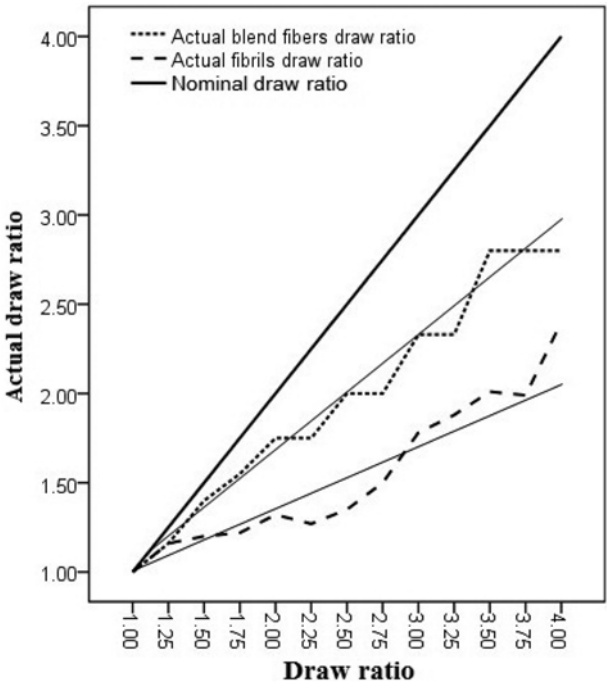

Fig. 7. Nominal and actual draw ratios of the blend fibres sample and nanofibres.

$$\text{Actual blend fiber draw ratio} = \left(\frac{\text{mean of undrawn blend fiber diameter}}{\text{mean of drawn blend fiber diameter}}\right) \quad (1)$$

The actual draw ratio of the fibrils was calculated by dividing the extracted fibril diameter mean of the undrawn fiber sample over the extracted fibrils diameter mean of the drawn fiber sample.

$$\text{Actual fibrils draw ratio} = \left(\frac{\text{mean of undrawn fiber diameter}}{\text{mean of drawn fiber diameter}}\right) \quad (2)$$

The maximum actual draw ratio of the blend fibers sample and the fibrils were 2.8 and 2.4, respectively. Nominal draw ratio and the best fitting lines of the actual draw ratios for the blend fibers sample and extracted fibrils are presented in Fig. 7.

As can be seen in Fig. 7, the actual draw ratios of the fibrils were much smaller than the actual draw ratios of the blend fiber sample as compared to their nominal draw ratios. This curve expresses that the draw ratio, which was applied by the drawing machine, was not completely transmitted to the fibers, and the actual draw ratio of the fibers sample was not completely transmitted to the fibrils. Therefore, a higher actual draw ratio is required for the fibers to produce thinner fibrils.

In this work, cold drawing operation was conducted; thus, the resulting difference between the nominal draw ratio and the actual draw ratio of the blend fibers sample may have had several causes such as:

1) Mechanical slippage of the blend fiber sample between the machine gauges due to incomplete contact of the outer surface of the fiber sample and the inner surface of the gauges.

2) Polymer chains tend to return to their original state after bringing out of the fibers from the machine gauge due to their very short stress-relaxation time.

3) Low stress transfer between the matrix phase and dispersed phase components of the blend fibers sample due to their immiscibility and low interface adhesion.

In another study [12], the researchers determined the amount of actual draw ratio by measuring the undrawn fiber diameter and drawn fiber diameter with the draw ratios of 1.3 and 2.6. In the former, the difference between the nominal and the actual draw ratio was reported as being 7.7%, while in the latter draw ratio, the difference was reported as being 36.9%. The difference in the present study was calculated as 7.2% in the draw ratio of 1.5 and 20% in the draw ratio of 2.5. In general, the difference increased by increasing the draw ratio, as is shown in Fig. 7. However, the difference obtained in this study was 20% lower than the difference obtained in another similar study [9]. These studies also reported the ratio of the average diameter of the undrawn PP fibrils and the average diameter of the drawn fibrils in the draw ratio of 2 to be equal to 1.2 [13]. The difference between the nominal and the actual draw ratio in the above mentioned draw ratio was 40%. Similarly, in the current study, the diameter ratio of the undrawn PP fibrils over the drawn fibrils in the draw ratio of 2 was equal to 1.32, and the difference was 34%. By comparing the results of the present work with previously cited research, it was shown that extracted nanofibrils from industrial-scale produced blend fibers were drawn with a higher amount of draw ratio rather than a laboratory-scale produced one [13].

To determine the relationship between the draw ratio and the

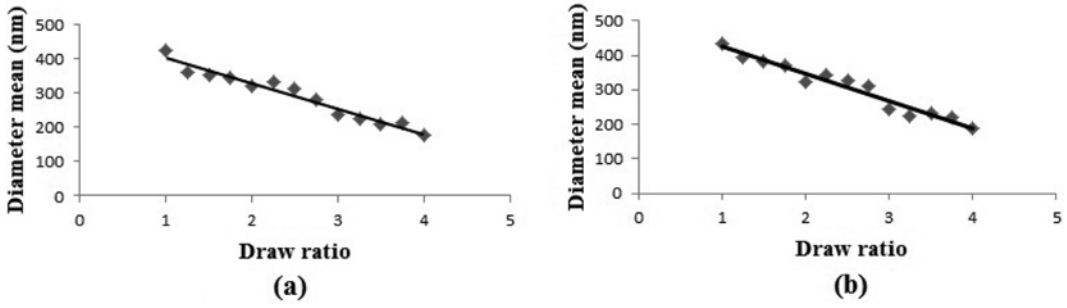

Fig. 8. Regression relationship between draw ratio and the mean of nanofibres diameters for: (a) Visual method, and (b) fuzzy c-means method.

diameter mean, the regression between the draw ratio and diameter was identified. The results of statistical regression are shown in Fig. 8 for the visual and the FCM methods.

The relationship for the visual method was obtained as regression coefficient (R) equal to 0.98 (R^2=0.9574), and the best fitting line equation can be shown as the following equation:

$$D_f = -73.901\ D.R + 475.04 \quad (3)$$

where D_f is the average of diameter (nm), and D.R is draw ratio. Also, according to the desired obtained confidence level, the variation trend between D_f and D.R was linear and indicated high effectiveness of draw ratio on diameter.

The relationship between the draw ratio and the mean of diameter using the FCM method is presented in Fig. 8(b). The relationship (R^2=0.9548) based on the best fitting line of D_f and D.R can be shown as:

$$D_f = -78.464\ D.R + 503.42 \quad (4)$$

where D_f is the average of diameter (nm), and D.R is draw ratio. From the mentioned results, it can be stated that the low difference between coefficients indicated good agreement between these two methods or expressing the relationship between draw ratio and diameter. Finally, it can be concluded that the image processing is a good alternative method instead of the conventional time-consuming visual method.

CONCLUSION

Producing nanofibers with high uniformity was possible via extraction from industrial-scale produced polymer blend fibers. By increasing the draw ratio of blend fibers, fibrils (dispersed phase component) became thinner while retaining good uniformity. The diameter uniformity of nanofibers extracted from industrial-scale-produced blend fibers was much higher than the diameter uniformity of nanofibers extracted from laboratory-scale produced blend fibers.

The deformation of fibrils was different in various elongations. The most changes of diameter with increasing the draw ratio occurred prior to the draw ratio of 2. The FCM method showed the highest correlation between the means of diameter which were measured by the various methods of thresholding. Comparing both of two diameter-determining methods by image processing (distance transform and direct tracking), with regard to the correlation results, the highest correlation was generally related to the distance transform method.

Morphological studies showed that the diameter of nanofibrils decreases by increasing the draw ratio. Closeness of the regression coefficients of the visual (R=0.98) and FCM methods (R=0.95) showed the suitability of the image processing method for determining the diameter of nanofibers. The mean of diameter for nanofibers extracted from the undrawn to drawn (D.R=4) PP/PBT blend fibers varied from 420 nm to 175 nm for the visual method and 435 nm to 188 nm for the FCM method. The actual draw ratios of the fibrils were much smaller than the actual draw ratios of the blend fiber sample and the nominal draw ratios. By increasing the draw ratio, the difference between the nominal draw ratio, actual draw ratio of the blend fiber sample and the actual draw ratio of the fibrils increased.

ACKNOWLEDGEMENT

The support of the Iran Nanotechnology Initiative Council is appreciated.

REFERENCES

1. M. A. Tavanaie, A. M. Shoushtari, F. Goharpey and M. R. M. Mojtahedi, *J. Polym. Sci. Tech. (in Persian)*, **5**, 367 (2008).
2. M. A. Tavanaie, A. M. Shoushtari and F. Goharpey, *J. Macromol. Sci., Part B, Phys.*, **49**, 1633 (2010).
3. M. V. Tsebrenko, A. V. Yudin, T. I. Ablazova and G. V. Vinogradov, *Polymer*, **17**, 831 (1976).
4. L. A. Utracki, M. M. Dumoulin and P. Toma, *Polym. Eng. Sci.*, **26**, 34 (1986).
5. A. D. Padsalgikar and M. S. Ellison, *Polym. Eng. Sci.*, **37**, 994 (1997).
6. Q. Xinga, M. Zhu, Y. Wang, Y. Chen, Y. Zhang, J. Piontech and Hs. Adler, *J. Polym.*, **46**, 5406 (2005).
7. M. A. Tavanaie, A. M. Shoushtari, F. Goharpey and M. R. M. Mojtahedi, *Fiber Polym.*, **14**, 396 (2013).
8. M. A. Tavanaie, A. M. Shoushtari and F. Goharpey, *The 1st International and the 7th National Iranian Textile Engineering Conference - Rasht, Iran*, Oct. (2009).
9. E. Bagheban Kochak, E. Fallahi and M. Haghighat Kish, *Iran. J. Polym. Sci. Tecnol. (in Persian),* **23**, 155 (2010).
10. K. Friedrich, M. Evstatiev, S. Fakirov, O. Evstatiev, M. Ishii and M. Harrass, *Compos. Sci. Technol.*, **65**, 107 (2005).
11. R. Zhao and C. L. Wadsworth, *Polym. Eng. Sci.*, **43**, 463 (2003).
12. E. Fallahi, M. Barmar and M. Haghighat Kish, *J. Appl. Polym. Sci.*, **108**, 1473 (2008).
13. E. Fallahi, M. Barmar and M. Haghighat Kish, *Iran. Polym. J.*, **20**, 433 (2011).
14. K. Jayanarayanan, T. Sabu and J. Kuruvilla, *Appl. Sci. Manuf.*, **39**, 164 (2008).
15. E. H. Shin, K. S. Cho, M. H. Seo and H. Kim, *Macromol. Res.*, **16**, 314 (2008).
16. M. Ziabari, V. Mottaghitalab and A. K. Haghi, *Korean J. Chem. Eng.*, **25**, 905 (2008).
17. M. Ziabari, V. Mottaghitalab, S. T. McGovern and A. K. Haghi, *Chin. Phys. Lett.*, **25**, 3071 (2008).
18. M. Ziabari, V. Mottaghitalab and A. K. Haghi, *Korean J. Chem. Eng.*, **28**, 751 (2011).
19. C. Zeyun, W. Rongwu, Z. Xianmiao and Y. Baopu, *Procedia. Eng.*, **15**, 3516 (2011).
20. M. Ziabari, V. Mottaghitalab and A. K. Haghi, *Korean J. Chem. Eng.*, **25**, 923 (2008).
21. A. H. Aydilek, S. H. Oguz and T. B. Edil, *J. Comput. Civil. Eng.*, **16**, 280 (2002).
22. M. A. Tavanaie, Ph.D. Thesis, Amirkabir University of Technology, Iran (2009).
23. N. Dehghan, P. Payvandy and M. A. Tavanaie, *J. Text. Sci. Technol. (in Persian)*, **3**, 17 (2014).

24. N. Dehghan, P. Payvandy and M. A. Tavanaie, *Int. J. Comput. Appl.*, **99,** 37 (2014).
25. K. S. Chuang, H. L. Tzeng, S. Chen, J. Wu and T. J. Chen, *Comput. Med. Imag. Grap.*, **30**, 9 (2006).
26. S. Sivakumar and C. Chandrasekar, *In Recent. Advances. Comput. Software. Systems (RACSS), International Conference on (109-113, IEEE, 2012).*
27. N. Dehghan, M. Sc. Thesis, Yazd University of Iran, February (2014).
28. M. Afshari, R. Kotek, M. Haghighat Kish, H. Nazock Dast and B. S. Gupta, *Polymer*, **43**, 1331 (2002).
29. J. S. Lee, K. H. Choi, H. D. Ghim, S. S. Kim, D. H. Chun, H. Y. Kim and W. S. Lyoo, *J. Appl. Polym. Sci.*, **93**, 1638 (2004).